doi:10.1016/j.gca.2004.05.038

Manganese(III) binding to a pyoverdine siderophore produced by a manganese(II)-oxidizing bacterium

DOROTHY L. PARKER,[1,*] GARRISON SPOSITO,[2] and BRADLEY M. TEBO[1]

[1]Marine Biology Research Division and Center for Marine Biotechnology and Biomedicine, Scripps Institution of Oceanography, University of California, San Diego, 9500 Gilman Drive, La Jolla, CA 92093-0202, USA
[2]Division of Ecosystem Sciences and Environmental Engineering Group, University of California, Berkeley, CA 94720-3100, USA

Abstract—The possible roles of siderophores (high affinity chelators of iron(III)) in the biogeochemistry of manganese remain unknown. Here we investigate the interaction of Mn(III) with a pyoverdine-type siderophore (PVD_{MnB1}) produced by the model Mn(II)-oxidizing bacterium *Pseudomonas putida* strain MnB1. PVD_{MnB1} confirmed typical pyoverdine behavior with respect to: (a) its absorption spectrum at 350–600 nm, both in the absence and presence of Fe(III), (b) the quenching of its fluorescence by Fe(III), (c) the formation of a 1:1 complex with Fe(III), and (d) the thermodynamic stability constant of its Fe(III) complex. The Mn(III) complex of PVD_{MnB1} had a 1:1 Mn:pvd molar ratio, showed fluorescence quenching, and exhibited a light absorption spectrum (A_{max} = 408–410 nm) different from that of either PVD_{MnB1}-Fe(III) or uncomplexed PVD_{MnB1}. Mn(III) competed strongly with Fe(III) for binding by PVD_{MnB1} in culture filtrates (pH 8, 4°C). Equilibration with citrate, a metal-binding ligand, did not detectably release Mn from its PVD_{MnB1} complex at a citrate/PVD_{MnB1} molar ratio of 830 (pH 8, 4°C), whereas pyrophosphate under the same conditions removed 55% of the Mn from its PVD_{MnB1} complex. Most of the PVD_{MnB1}-complexed Mn was released by reaction with ascorbate, a reducing agent, or with EDTA, a ligand that is also oxidized by Mn(III). Data on the competition for binding to PVD_{MnB1} by Fe(III) vs. Mn(III) were used to determine a thermodynamic stability constant (nominally at 4°C) for the neutral species $MnHPVD_{MnB1}$ (log K = 47.5 ± 0.5, infinite dilution reference state). This value was larger than that determined for $FeHPVD_{MnB1}$ (log K = 44.6 ± 0.5). This result has important implications for the metabolism, solubility, speciation, and redox cycling of manganese, as well as for the biologic uptake of iron. *Copyright © 2004 Elsevier Ltd*

1. INTRODUCTION

In nature, manganese occurs in three oxidation states: Mn(II), which can exist as a soluble ion, and Mn(III) or Mn(IV), which are found typically as insoluble Mn(III, IV) minerals. Soluble Mn(III) has been thought to be rare in natural waters because it should hydrolyze and precipitate as Mn(III) oxides or disproportionate into Mn(IV) oxides plus Mn(II) (Nealson et al., 1988; Nealson et al., 1989; Stumm and Morgan, 1996) unless stabilized in complexes with ligands such as oxalate (Stone, 1987; Xyla et al., 1992; Hatakka, 1994), pyrophosphate (Kostka et al., 1995; Klewicki and Morgan, 1998) and perhaps citrate, which forms a relatively long-lived Mn(III) complex at pH > 7 (Klewicki and Morgan, 1998; Luther et al., 1998). Manganese(III) complexes participate as intermediates in fungal degradation of phenolic compounds (Popp et al., 1990; Perie and Gold, 1991; Dutton and Evans, 1996; Call and Mucke, 1997; Leonowicz et al., 2001; Schlosser and Hofer, 2002; Hatakka et al., 2003) and in bacterial respiration of organic substrates in anaerobic environments (Kostka et al., 1995; Tebo et al., 1997). Bacterial oxidation of Mn(II) to Mn(IV) has been recently shown to involve an Mn(III) intermediate (Webb et al., 2002), which is consistent with the known electron-transfer mechanisms of the multicopper oxidases required for this process (van Waasbergen et al., 1993; van Waasbergen et al., 1996; De Vrind et al., 1998; Brouwers

et al., 1999; Brouwers et al., 2000; Francis and Tebo, 2001; Francis et al., 2002).

Among the most prevalent of the Mn(II)-oxidizing bacteria are the fluorescent *Pseudomonas* species, such as *P. putida,* that occur in diverse habitats worldwide (Tebo et al., 1997; Francis and Tebo, 2001). The poorly-crystalline layer type Mn oxide produced by *P. putida* strain MnB1 has been characterized by Villalobos et al. (2003), who found that it contains both Mn(III) and Mn(IV), although Mn(IV) predominates. When iron-starved, fluorescent pseudomonads produce a class of siderophores called pyoverdines (PVDs), which strongly chelate Fe(III) in a 1:1 complex that interacts with a specific cellular receptor to promote iron uptake by the organism (Demange et al., 1987; Budzikiewicz, 1993; Albrecht-Gary et al., 1994; Kisaalita et al., 1997; Albrecht-Gary and Crumbliss, 1998; Meyer, 2000; Folschweiller et al., 2002; Schalk et al., 2002). Pyoverdine's metal-binding site, comprising two hydroxamate groups and one catecholate group, also includes a dihydroxyquinoline-containing fluorochromophore that shows altered light absorption and fluorescence in response to Fe(III) binding. The neutral complex FeHPVD° is the predominant PVD-Fe(III) species at pH 6–10 (Albrecht-Gary et al., 1994).

Pseudomonas putida mutants that constitutively produce PVDs also exhibit reduced oxidation of Mn(II) to Mn(IV) (Caspi et al., 1998; De Vrind et al., 1998). Furthermore, *P. putida* strains show retarded Mn(IV) production when limited for iron (i.e., when PVD is produced), suggesting that Mn(II) oxidation either requires Fe or is inhibited by PVD (B. M. Tebo, K. J. Murray and R. Verity, unpublished data). Here we report an additional link between PVD

* Author to whom correspondence should be addressed (doparker@ucsd.edu).

and Mn(II) oxidation, namely that a PVD produced by the model Mn(II)-oxidizing bacterium *P. putida* MnB1 binds Mn(III) at least as strongly as it does Fe(III), making it the highest-affinity naturally-occurring ligand of Mn(III) reported to date. This result has immediate implications concerning: (a) the effects of PVD on microbial oxidation of Mn(II) to Mn(IV) via a Mn(III) intermediate, (b) the influence of oxidized Mn on siderophore-mediated uptake of Fe(III) by microbes, and (c) the solubilization and stabilization of Mn(III) by siderophores in the environment.

2. MATERIALS AND METHODS

2.1. Culture Filtrate

Effects of iron on pyoverdine biosynthesis were examined in parallel cultures of *Pseudomonas putida* strain MnB1 (Schweisfurth, 1973) that were propagated either with or without 10 μM $FeSO_4$ in minimal salts pyruvate (MSP) medium containing (g/L): $(NH_4)_2SO_4$, 0.24; $MgSO_4 \cdot 7H_2O$, 0.06; $CaCl_2 \cdot 2H_2O$, 0.06; KH_2PO_4, 0.02; Na_2HPO_4, 0.3; and Na pyruvate, 0.8. All subsequent experiments utilized aliquots of a single culture (5×10^7 cells/mL) of strain MnB1 which was grown for 18 h at 25°C in MSP medium lacking added Mn or Fe. The pH value was initially set at 7.4 with 10 mM HEPES (Na N-(2-hydroxyethyl) piperazine-N′-(2-ethanesulfonate)) buffer, but rose to 7.8 at the end of growth. After this growth period, the culture was centrifuged and the supernatant solution was aseptically filtered (0.45 μm Gelman GN-6 filter). Aliquots of the filtrate were frozen at −20°C. Aliquots were thawed, supplemented with a buffer (67 mM HEPES buffer at pH 8 or 0.1 M Na acetate solution at pH 5), and mixed with 1 mL of CHELEX-100 resin (BioRad Analytical Grade, Na-form, 142-2832, 0.4 mol$_c$/L) that had been equilibrated in that buffer. The mixture was shaken intermittently for 10–17 h at 4°C, passed through a column of CHELEX-100 resin to remove divalent cations (Mg^{2+} and Ca^{2+}) of the growth medium, eluted with the buffer, and filtered (0.2 μm pore size Acrodisk filter). CHELEX-100 treatment was omitted in a few cases ("raw" samples). For brevity, the PVD-containing culture filtrate is designated PVD_{MnB1}.

Aldrich reagent-grade or Sigma Ultra-Pure chemicals were prepared in MilliQ deionized water and pH-adjusted with NaOH or HCl. Fe(III)-containing stock solutions were: (a) 500 μM $FeCl_3$ in deionized water, (b) 1 mM Fe(III) citrate in 67 mM HEPES buffer at pH 8, and (c) citrate-chelated Fe(III) (citrate-Fe(III)) containing 1 mM Fe(III) citrate, 20 mM sodium citrate, and 3 mM sodium acetate in 67 mM HEPES buffer at pH 8. Freshly-prepared manganese stock solutions were: (a) 1–3 mM Mn(III) acetate in absolute ethanol, (b) citrate-chelated Mn(III) (citrate-Mn(III)) containing 1 mM Mn(III) acetate and 20 mM sodium citrate in 67 mM HEPES buffer at pH 8, and (c) citrate-chelated Mn(II) (citrate-Mn(II)) containing 1 mM Mn(II) acetate and 20 mM sodium citrate in 67 mM HEPES buffer at pH 8. The names of simple salts (e.g., Fe(III) citrate) are written without a hyphen and with the metal first, whereas strong complexes or chelates (e.g., citrate-Fe(III)) are designated with a hyphen and with the citrate first.

Immediately before each experiment, the Mn(III) concentration in freshly-prepared Mn(III) acetate or citrate-Mn(III) stock solutions was determined from absorbance at 320 or 430 nm (Klewicki and Morgan, 1998). Sodium EDTA (1, 10, or 50 mM, pH 8) was reacted for >30 min with samples of CHELEX-treated or "raw" (not CHELEX-treated) culture filtrate (PVD_{MnB1}) in either 0.1 M sodium acetate buffer at pH 5 or 67 mM HEPES buffer at pH 8. CHELEX-, EDTA-, and untreated samples (5–18 μM PVD_{MnB1}) at pH 5 or pH 8 were exposed to varying concentrations (10 and 50 μM) of $FeCl_3$, Fe(III) citrate, citrate-Fe(III) chelate, citrate-Mn(III) chelate, or Mn(III) acetate. Absorption spectra (320–600 nm, section 2.5) and fluorescence intensities (section 2.6) of the various samples were obtained after 20–24 h equilibration at 4°C.

The PVD concentration in the Fe-, EDTA-, or CHELEX-treated samples was calculated from published molar extinction coefficients, ε, (Meyer and Abdallah, 1978; Demange et al., 1987) of PVD-Fe(III) (400 nm, $\varepsilon = 19,000$ M^{-1} cm^{-1}; 460 nm, $\varepsilon = 6500$ M^{-1} cm^{-1}) or iron-free PVD (400 nm, $\varepsilon = 20,500$ M^{-1} cm^{-1} at pH 8; 382 nm, $\varepsilon = 16,500$ M^{-1} cm^{-1} at pH 5). The PVD_{MnB1} concentrations in Fe(III), EDTA, and CHELEX controls were averaged; experimental data were

divided by this mean value to calculate molar extinction coefficients of experimental samples at various wavelengths. The PVD_{MnB1} concentrations in raw samples were determined from empiric extinction coefficients (Section 3.1.1) and confirmed by comparison to identically-diluted aliquots that had been saturated with Fe(III) or with 10–50 mM EDTA.

2.2. Competition of EDTA and PVD_{MnB1} for Fe(III)

Raw PVD_{MnB1} (12 $\pm$ 1 μM) at pH 8 in 67 mM HEPES buffer containing 10 μM Fe(III) citrate and 30 μM sodium acetate was equilibrated at 4°C for 26 to 27 h and then supplemented with sodium EDTA (pH 8) to 0, 1, or 10 mM. Triplicate 100 μL aliquots were dispensed into Falcon (35-3296) microtiter plates, which were sealed and equilibrated at 4°C. Fluorescence intensity at 4°C (section 2.6) was measured at timed intervals. At each time point, data were normalized to the fluorescence of PVD_{MnB1} that contained 10 mM EDTA but no added Fe(III).

2.3. Mn(III) Complex of PVD_{MnB1}

2.3.1. Absorbance and Fluorescence

Metal-containing stock solutions were prepared as in section 2.1. Citrate-Mn(III), citrate-Mn(II), and citrate-Fe(III) were diluted in 20 mM Na citrate (pH 8) to form solutions of 0.02–2 mM Mn(III), Mn(II), or Fe(III); these solutions were then diluted 1/20 into samples of CHELEX-treated PVD_{MnB1} (8.5 $\pm$ 0.7 μM) or raw PVD_{MnB1} (8.5 $\pm$ 1 μM), each containing 1 mM Na citrate and 67 mM HEPES buffer at pH 8. Mn(III) acetate (3 mM in absolute ethanol) was appropriately diluted into CHELEX-treated PVD_{MnB1} (8.5 $\pm$ 1.6 μM in 67 mM HEPES buffer at pH 8, no citrate) and examined in parallel with the citrate-containing mixtures. The blank for each PVD_{MnB1}-containing sample was an identically supplemented and handled sample of uninoculated MSP medium. Samples with varying concentrations of citrate-Mn(III), citrate-Mn(II), citrate-Fe(III), or Mn(III) acetate were equilibrated at 4°C for 3 h, filtered through 0.2 μm Acrodisk filters, then further equilibrated at 4°C in the absence of light in sealed microfuge tubes (absorbance measurements) or sealed Falcon (35-3296) microtiter plates (fluorescence measurements). The fluorescence intensity at 4°C (section 2.6) of triplicate samples was measured after 23 h equilibration. Absorption spectra (section 2.5) were obtained after 3, 22, and 24 h; however, spectra obtained at all three time points were identical. The spectra of aliquots that had been filtered twice at 3 and 21 h did not differ from those filtered only once at 3 h. To investigate the effect of EDTA on a PVD_{MnB1}-Mn(III) complex that had been equilibrated with citrate-Mn(III) for 20 h at 4°C, 10 mM EDTA was added at 20 h; the EDTA-containing sample was equilibrated for 10 additional hours and its absorption spectrum was determined.

Citrate-Mn(III) or Mn(III) acetate background absorbance was subtracted from all data. However, the molar extinction coefficients (ε) of citrate-Mn(III) or Mn(III) acetate were much smaller at pertinent wavelengths than were those of PVD_{MnB1} or its Fe(III) or Mn(III) complexes (PVD_{MnB1}-Fe(III) or PVD_{MnB1}-Mn(III)). At pH 8, the value of ε at 400 nm for citrate-Mn(III), MnIII acetate, PVD_{MnB1} or PVD_{MnB1}-Fe(III) was 165, 137, 20,500, or 19,000 M^{-1} cm^{-1}, respectively; that at 410 nm for citrate-Mn(III), Mn(III) acetate, or PVD_{MnB1}-Mn(III) was 200, 130, or 17,000 M^{-1} cm^{-1}, respectively; that at 460 nm for citrate-Mn(III), Mn(III) acetate, or PVD_{MnB1}-Fe(III) was 182, 82, or 6500 M^{-1} cm^{-1}, respectively.

2.3.2. Citrate effects on the reaction of Mn(III) with PVD_{MnB1}

Mn(III) acetate or citrate-Mn(III) chelate was added to PVD_{MnB1} in 67 mM HEPES buffer at pH 8; final concentrations were 50 μM Mn and 13.5 μM PVD_{MnB1}. The fluorescence intensity (section 2.6) of triplicate samples was measured at timed intervals during equilibration at 4°C.

2.3.3. Stability in the presence or absence of competing ligands or reductants

2.3.3.1. Citrate, pyrophosphate, EDTA. 1 mM Mn (III) acetate in absolute ethanol was diluted 1/100 into 12 $\pm$ 1 μM raw

PVD_{MnB1} in 67 mM HEPES buffer at pH 8. The mixture was equilibrated at 4°C until competing ligands (pH 8) were added to it and to a parallel sample without Mn(III). Ligands were added at the following times: 20 h, 10 mM sodium citrate; 1 mM $Na_4P_2O_7$; 45.6 h, 10 mM $Na_4P_2O_7$. Quadruplicate 100 μL samples were equilibrated at 4°C in sealed microtiter plates and fluorescence intensity was examined at timed intervals. At 75–76 h, 10 mM EDTA (pH 8) was added to half of the microtiter wells containing each mixture; an equal volume (5 μL) of pH 8 water was added to each of the other wells. Fluorescence intensity at each time point was normalized to that of PVD_{MnB1} controls without Mn(III) but with the same competing ligand(s) and other supplements.

2.3.3.2. Ascorbate. 1 mM Mn(III) acetate in absolute ethanol was diluted 1/50 into 12 ± 1 μM raw PVD_{MnB1} in 67 mM HEPES buffer at pH 8. After 1 h at 25°C, half was supplemented with 1 mM sodium ascorbate. Sealed samples then were equilibrated for 1 h at 25°C and their fluorescence intensity measured at 4°C, with normalization to a parallel PVD_{MnB1} sample that contained ascorbate but lacked Mn(III).

2.4. Competition of Fe(III) and Mn(III) for PVD_{MnB1}

2.4.1. Simultaneous addition of citrate-Fe(III) and citrate-Mn(III)

Citrate-Fe(III) and citrate-Mn(III) (section 2.1) were diluted into 20 mM sodium citrate (pH 8) to make mixtures containing: 100 μM Fe with 0, 100, or 120 μM Mn; 200 μM Fe with 0, 100, 120, or 150 μM Mn; 100 μM Mn with 0, 100, 300, or 500 μM Fe; 200 μM Mn with 0, 400, or 1200 μM Fe; no Mn or Fe. Each mixture (100 μL) was added to 900 μL CHELEX-treated PVD_{MnB1} (8.1 ± 0.9 μm final concentration) in 1 mM sodium citrate and 67 mM HEPES buffer at pH 8. Samples were filtered (0.22 μm pore size, Acrodisk) after 19 h equilibration at 4°C in sealed microfuge tubes; absorption spectra were determined at 20 and 41 h. The blank for each PVD_{MnB1}-containing sample was an identically supplemented and handled sample of uninoculated MSP medium. α_{FeL} (the mole fraction of PVD-Fe(III) relative to total PVD) was calculated from absorbance at 460 nm (section 2.7).

2.4.2. Sequential addition of citrate-Fe(III) and citrate-Mn(III)

At 0 h, citrate-Fe(III) (10 μM), citrate-Mn(III) (10 μM), or a mixture of citrate-Fe(III) plus citrate-Mn(III) (each 10 μM) was added to 8.1 ± 0.9 μM PVD_{MnB1} in 2 mM sodium citrate and 67 mM HEPES buffer at pH 8, in duplicate. After 19 h equilibration at 4°C, portions of each sample were filtered (0.22 μm pore size Acrodisk) and absorption spectra were determined. At 20 h, the unfiltered aliquots were supplemented as follows: citrate-Fe(III) (10 μM) was added to one of the two samples with citrate-Mn(III); citrate-Mn(III) (10 μM) was added to one of the two samples with citrate-Fe(III); an equal volume of HEPES buffer was added to the other samples. All samples were equilibrated at 4°C and filtered at 40 h (20 h after the second additions); absorption spectra of iced samples were determined at 41 h. The blank for each PVD_{MnB1}-containing sample was an identically supplemented and handled sample of uninoculated MSP medium. α_{FeL} was calculated from absorbance as described in section 2.7. $\alpha_{FeL} = 1$ based on the average absorbance at 460 nm (A_{460}) of the two Fe-only samples at 19 h; $\alpha_{FeL} = 0$ was based on the average A_{460} of the two Mn-only samples at 19 h. Within each set of duplicates, A_{460} values at 19 h differed by <2%.

2.5. Absorbance Measurements

Samples equilibrated for ≥3 h at 4°C in sealed microfuge tubes were passed through 0.2 μm pore size Acrodisk filters and transferred to 500-μL quartz cuvettes (1 cm optical pathlength). Absorbance at 3 nm intervals between 320 and 600 nm was determined with a Perkin-Elmer Bio20 UV-VIS spectrophotometer. The blank for each PVD_{MnB1}-containing sample was an identically supplemented and handled sample of uninoculated MSP medium. Until transfer to a cuvette, each sample was kept at 4°C.

2.6. Fluorescence Emission Measurements

Unless otherwise stated, all samples were equilibrated and examined at 4°C. Fluorescence excitation and emission spectra were determined with an ISA FluoroMax 2 scanning fluorimeter. Fluorescence quenching experiments utilized a Perkin-Elmer HTS7000 plate reader. Conditions at pH 8 in 67 mM HEPES buffer were: excitation at 405 nm, emission at 535 nm, gain = 50. Conditions at pH 5 in 0.1 M sodium acetate were: excitation at 360 nm, emission at 595 nm, optimal gain. After preliminary reaction for ≥3 h in microfuge tubes, experimental mixtures were passed through 0.2 μm pore size Acrodisk filters and 100 μL samples were equilibrated at 4°C in sealed white microtiter plates (Falcon 35-3296) in the absence of light. Unless otherwise indicated, measurements were made on triplicate samples. Fluorescence intensity (I) was corrected for a small (<0.3% I) background fluorescence of parallel samples in uninoculated MSP medium and for the residual fluorescence of metal-saturated samples (I^o_{ML}); it was then normalized to the similarly corrected fluorescence of parallel samples without added metal ($I^o - I^o_{ML}$). Coefficients of variations of replicate mixtures were typically <4% and those of replicate samples from the same mixture were <1%. The plate reader gave relative fluorescence intensity $[(I - I^o_{ML})/(I^o_L - I^o_{ML})]$ readings that differed by <10% from those taken on the scanning fluorimeter under the same conditions.

2.7. Data Analysis

The molar ratio of bound Fe or Mn (α_{ML}) is defined as

$$\alpha_{ML} = [ML]/[L_{TOTAL}] \quad (M = Fe \text{ or } Mn) \tag{1}$$

where L is PVD_{MnB1} and ML is a PVD_{MnB1} complex with either Fe or Mn. The value of α_{ML}, quantified by absorbance at 460 nm (for Fe in either the presence or absence of Mn) or by fluorescence quenching (for either Fe or Mn alone), was calculated with conventional formulas (Ryan and Weber, 1982; Blaser and Sposito, 1987):

$$\alpha_{ML} = ((A/A^o_L) - 1)/((A^o_{ML}/A^o_L) - 1) = (A - A^o_L)/(A^o_{ML} - A^o_L) \tag{2}$$

$$\alpha_{ML} = (1 - (I/I^o_L))/(1 - (I^o_{ML}/I^o_L)) = (I^o_L - I)/(I^o_L - I^o_{ML}) \tag{3}$$

where A is absorbance and I is fluorescence emission intensity. The absorbance of a solution containing only ligand is denoted A^o_L, whereas that of a solution containing only metal-saturated ligand is denoted A^o_{ML}, with similar definitions of I^o_L and I^o_{ML}. To interpret fluorescence data that are plotted as $(I - I^o_{ML})/(I^o_L - I^o_{ML})$, it should be noted that:

$$(I - I^o_{ML}) = (I^o_L - I^o_{ML}) - (I^o_L - I) \tag{4}$$

Dividing both sides of eqn. 4 by $(I^o_L - I^o_{ML})$ and substituting eqn. 3 yields:

$$(I - I^o_{ML})/(I^o_L - I^o_{ML}) = 1 - \alpha_{ML} \tag{5}$$

The value of A^o_{FeL}/A^o_L at 460 nm was 13 ± 1 (triplicate measurements in each of two experiments with 8.1 and 8.5 μM CHELEX-treated PVD_{MnB1} at pH 8). The value of I^o_{ML}/I^o_L of CHELEX-treated PVD_{MnB1} was 0.17 ± 0.03 with citrate-Fe(III) or 0.16 ± 0.02 with citrate-Mn(III) (quadruplicate measurements as duplicates from two independent experiments) and did not depend on PVD_{MnB1} concentration in the range investigated (8–19 μM).

Forward modeling (simulation) using the program MINEQL+ (Schecher and McEvoy, 1998) was applied to interpret the results quantitatively. The PVD_{MnB1}-EDTA competition experiments (sections 2.2 and 3.2) were simulated using the Fe(III) citrate, EDTA, and hydrolysis data in Table 1, but with the value of the log thermodynamic stability constant for the complex, $FeHPVD_{MnB1}$ (the dominant Fe(III)-pyoverdine species at pH 8; Albrecht-Gary et al., 1994) treated as an adjustable parameter to fit α_{FeL} data. Under the assumption that Fe(III) and Mn(III) formed identical complexes with acetate and citrate, the Fe(III)-Mn(III) competition experiments (sections 2.4 and 3.4) then were simulated using the acetate, citrate and hydrolysis data in Table 1 and the value of the adjusted log thermodynamic stability constant for $FeHPVD_{MnB1}$, but with the value of the log thermodynamic stability constant for the expected complex, $MnHPVD_{MnB1}$ treated as an adjust-

Table 1. Thermodynamic stability constants used in forward simulations.

Ligand (cation(s))	$\log \beta_{abcd}$[a] (a = metal, b = ligand c = H^+, d = OH^-)	Reference
$Citrate^{3-}$ (H^+) 25°C	$\log \beta_{0110} = 6.396$ $\log \beta_{0120} = 11.157$ $\log \beta_{0130} = 14.285$	Martell et al. (1998)
$Citrate^{3-}$ (Fe^{3+}, H^+) 25°C	$\log \beta_{1110} = 14.40$ $\log \beta_{1101} = 10.01$ $\log \beta_{1200} = 19.16$ $\log \beta_{1210} = 23.45$ $\log \beta_{1220} = 26.35$ $\log \beta_{1201} = 14.48$ $\log \beta_{1202} = 6.58$ $\log \beta_{1203} = -0.27$	Ribas et al. (1989)
OH^- (Fe^{3+}) 25°C	$\log^* \beta_{1001} = -2.2$ $\log^* \beta_{1002} = -4.6$ $\log^* \beta_{1004} = -21.6$ $\log^* \beta_{2002} = -2.9$ $\log^* \beta_{3004} = -6.3$	Martell et al. (1998)
OH^- (Mn^{3+}) 25°C	$\log^* \beta_{1001} = 0.4$ $\log^* \beta_{1002} = 0.5$	Martell et al. (1998)
$EDTA^{4-}$ (H^+, Fe^{3+}) 25°C	$\log \beta_{0110} = 10.948$ $\log \beta_{0120} = 17.221$ $\log \beta_{0130} = 20.341$ $\log \beta_{0140} = 24.557$ $\log \beta_{0150} = 26.057$ $\log \beta_{0160} = 24.268$ $\log \beta_{1100} = 27.682$ $\log \beta_{1110} = 29.199$ $\log \beta_{1101} = 19.984$ $\log \beta_{1102} = 41.768$	Martell et al. (1998)
$Acetate^-$ (H^+, Fe^{3+}) 25°C	$\log \beta_{0110} = 4.757$ $\log \beta_{1100} = 4.023$ $\log \beta_{1200} = 7.572$ $\log \beta_{1300} = 9.58$	Martell et al. (1998)
$Pyoverdine^{4-}$ (H^+) 25°C	$\log \beta_{0110} = 12.2$ $\log \beta_{0120} = 23.0$ $\log \beta_{0130} = 30.6$ $\log \beta_{0140} = 39.2$ $\log \beta_{1050} = 44.9$ $\log \beta_{0160} = 49.7$	Albrecht-Gary et al. (1994)
$Pyoverdine^{4-}$ (Fe^{3+}, H^+) 25°C	$\log \beta_{1100} = 47.8$ $\log \beta_{1110} = 43.0$ $\log \beta_{1120} = 30.8$	Albrecht-Gary et al. (1994)

[a] Formation of $M_aH_cOH_dL_b$ from free-ion reactants. Values were adjusted to infinite dilution (section 2.7) but were not corrected to 4°C (Ribas et al., 1989; Martell et al., 1998).

able parameter to fit α_{MnL} data. Finally, the metal-addition experiments (sections 2.1, 3.1, 2.3, and 3.3) were simulated using the log thermodynamic complex stability constants for $FeHPVD_{MnB1}$ and Mn-$HPVD_{MnB1}$ along with those listed in Table 1. If necessary, complex stability constants selected from the references given in Table 1 were corrected to infinite dilution using the Davies Equation (Sposito, 1989), but they were not corrected to 4°C because pertinent standard enthalpies were unknown in many cases.

3. RESULTS AND DISCUSSION

3.1. Properties of Culture Filtrates

3.1.1. Absorption spectra

Filtrates of supernatant fluids from iron-limited cultures—but not parallel iron-replete cultures—of *Pseudomonas putida* strain MnB1 exhibited spectra that strikingly resembled those

of pyoverdine-type (PVD) siderophores, absorbing light strongly at 380 nm at pH 5 or 400–402 nm at pH 8 (Table 2). To study this phenomenon under physiologically relevant conditions, the filtered culture medium (PVD_{MnB1}) from a chromophore-containing culture that had been grown without added Fe or Mn was examined after minimal dilution (1.2- to 4-fold) by buffer and reagents. At either pH 5 or 8, the addition to PVD_{MnB1} of excess $FeCl_3$, Fe(III) citrate, or Fe(III) chelated with 20 times more sodium citrate that Fe(III) citrate (citrate-Fe(III), section 2.1) yielded the characteristic spectrum of PVD-Fe(III), i.e., maximal absorption at 400–402 nm with shoulders at 460 nm and 540 nm (Fig. 1) (Demange et al., 1987; Albrecht-Gary et al., 1994). The absorbance ratios A_{460}/A_{540} and A_{460}/A_{400} for Fe(III)-saturated PVD_{MnB1} were in good agreement with published values for PVD-Fe(III) (Table 2). The ratio A_{460}/A_{400} of untreated PVD_{MnB1} was no greater than that predicted for iron-free PVD (PVD) and was an order of magnitude smaller than that of PVD-Fe(III) (Table 2). In general, the spectrum of untreated PVD_{MnB1} did not differ substantially from that of iron-free PVD. However, treatment with either a metal chelator (10 mM EDTA) or the cation exchange resin CHELEX-100 (which was expected to exchange Mg^{2+}, Ca^{2+} or trace metal contaminants in the culture medium for sodium) shifted the absorbance maximum at pH 8 from 402 to 400 nm, slightly decreased A_{408}/A_{400}, and increased A_{400} by $3.9 \pm 0.3\%$ (Table 2; Fig. 2, curves 4 and 6). We conclude that the predominant chromophore in the culture filtrate is iron-free PVD_{MnB1} that shows the expected pH effect on its absorption spectrum and yields the typical PVD-Fe(III) spectrum in the presence of excess Fe(III) (Table 2, Fig. 1 and 2). The minor changes in the raw PVD_{MnB1} spectrum after treatment with EDTA or CHELEX may suggest the binding by PVD_{MnB1} of metal(s) from the growth medium. These metals could be largely displaced by Fe(III), since the spectra of both raw and CHELEX-treated PVD_{MnB1} were identical after exposure to Fe(III) (Fig. 1).

The pyoverdine concentration in undiluted PVD_{MnB1}, based on published molar extinction coefficients (Meyer and Abdallah, 1978; Demange et al., 1987) and known dilution factors, was similar irrespective of whether it was calculated from measurements at pH 5 ($20.6 \pm 0.6 \mu M$, eight spectra of Fe(III)- or CHELEX-treated PVD_{MnB1}) or pH 8 ($20.9 \pm 1.2 \mu M$, seven spectra of Fe(III)- or CHELEX-treated PVD_{MnB1}). Concentration values also agreed for PVD_{MnB1}-Fe(III) ($20.0 \pm 1.2 \mu M$, eight spectra, pH 5 or 8) and raw PVD_{MnB1} ($21.4 \pm 1.1 \mu M$, seven spectra at pH 8, empiric ε at 400 nm, Fig. 2). The mean of all measurements ($20.7 \mu M$) was used in subsequent calculations.

3.1.2. Fluorescence intensity

The molar fluorescence intensity of CHELEX-treated or raw PVD_{MnB1} was, respectively, $1.9 \pm 0.05 \times 10^9$ or $1.8 \pm 0.1 \times 10^9$ plate reader units at pH 8 (excitation at 405 nm and emission read at 535 nm, 4°C). The fluorescence was quenched by the addition of Fe(III) citrate, consistent with the known effects of Fe(III) on pyoverdine fluorescence (Budzikiewicz, 1993; Kisaalita et al., 1997; Meyer, 2000; Folschweiller et al., 2002). The calculated mole fraction of PVD_{MnB1}-Fe(III) (α_{FeL}) as a function of added Fe at pH 8 and 4°C was similar irrespective of whether fluores-

Table 2. Absorbance ratios of PVD$_{MnB1}$ at 4°C in comparison to those of a typical PVD, pyoverdine PaA.[a]

Pyoverdine	Absorbance ratio at specified wavelengths[b]					λ$_{max}$ [shoulder] (nm)
	A$_{460}$/A$_{380}$	A$_{460}$/A$_{400}$	A$_{364}$/A$_{380}$	A$_{400}$/A$_{380}$	A$_{460}$/A$_{540}$	
PVD, pH 5, no Fe						
PaA[a]	0.030		(0.97) 0.89	0.41		380 [364]
MnB1, EDTA treated	0.025 ± 0.003		0.96 ± 0.05	0.43 ± 0.01		380 [364]
MnB1, CHELEX treated	0.026 ± 0.002		0.96 ± 0.02	0.43 ± 0.02		380 [364]
PVD, pH 8, no Fe						
PaA[a]		0.030		1.29		403 [382]
MnB1, raw		0.028 ± 0.003		1.24 ± 0.2		402 [382]
MnB1, EDTA treated		0.029 ± 0.003		1.24 ± 0.04		400 [382]
MnB1, CHELEX treated		0.028 ± 0.003		1.15 ± 0.6		400 [382]
MnB1, CHELEX & EDTA treated		0.029 ± 0.002		1.26 ± 0.3		400 [382]
PVD-Fe(III)						
PaA, pH 5 or 8[a]		0.33		1.21	0.53	403 [460]
MnB1, raw, pH 5		0.32 ± 0.02		1.19 ± 0.02	0.51 ± 0.03	400 [460]
MnB1, CHELEX treated, pH 5		0.32 ± 0.02		1.18 ± 0.01	0.52 ± 0.04	400 [460]
MnB1, raw, pH 8		0.33 ± 0.02		1.17 ± 0.02	0.53 ± 0.04	398 [460]
MnB1, CHELEX treated, pH 8		0.33 ± 0.01		1.11 ± 0.03	0.53 ± 0.02	398 [460]

[a] Measured on enlarged photocopies of figure 2 in Albrecht-Gary et al. (1994). Values in parentheses were calculated from molar extinction coefficients in Demange et al. (1987).
[b] Mean ± standard deviation of triplicate or quadruplicate measurements at the absorbance maximum near 400 or 380 nm (400–403 nm or 380–382 nm).

cence or light absorption data were used (Fig. 3). A break in that curve (Fig. 3) occurred near the expected 1:1 mol/L ratio of added Fe to PVD$_{MnB1}$, thus confirming the PVD concentrations that were calculated from molar extinction coefficients (section 3.1.1).

3.2. Competition between EDTA and PVD$_{MnB1}$ for Fe(III)

The conditional stability constant (K$_{PVD}$) of the PVD$_{MnB1}$-Fe(III) complex in a culture filtrate containing 12 μM PVD$_{MnB1}$

and 10 μM Fe(III) at pH 8 (4°C) was determined by conventional EDTA competition (Meyer and Abdallah, 1978; Ongena et al., 2002). The 37–71 h data from both 1 mM and 10 mM EDTA-containing mixtures (Fig. 4) were analyzed to obtain the concentration of PVD$_{MnB1}$-Fe(III) [PVD-Fe] and K$_{PE}$, the conditional equilibrium constant of the competition reaction:
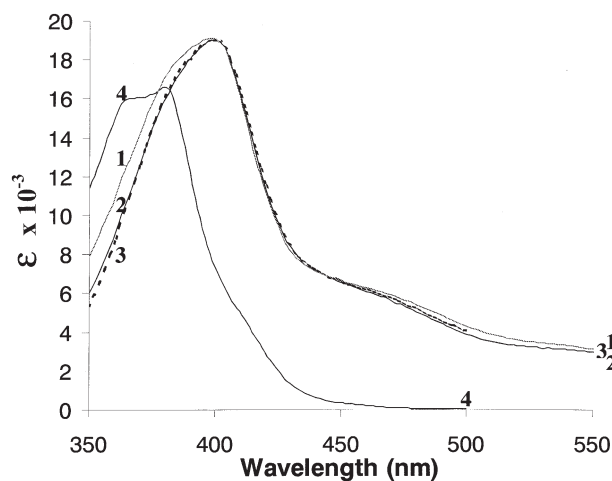

Fig. 1. Molar extinction coefficient (ε) of raw or CHELEX-pretreated PVD$_{MnB1}$ in the presence or absence of Fe(III) after 20–24 h equilibration at 4°C: (1) PVD$_{MnB1}$-Fe(III) complex at pH 8, formed with 8.5 μM CHELEX-pretreated PVD$_{MnB1}$ and 30 μM Fe(III) added as citrate-Fe(III) (citrate-chelated Fe(III), section 2.1); (2) PVD$_{MnB1}$-Fe(III) complex at pH 5, formed with 17.4 μM raw PVD$_{MnB1}$ and 50 μM FeCl$_3$; (3) PVD$_{MnB1}$-Fe(III) complex at pH 5, formed with 5 μM CHELEX-pretreated PVD$_{MnB1}$ and 30 μM FeCl$_3$; (4) 5 μM CHELEX-pretreated PVD$_{MnB1}$ at pH 5 with no added Fe(III).
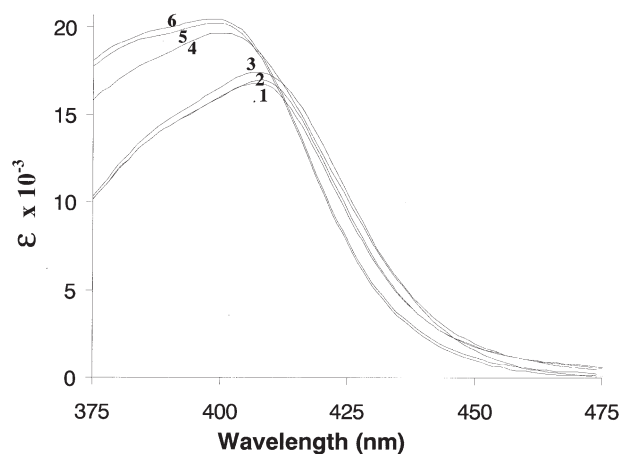

Fig. 2. Molar extinction coefficient (ε) at pH 8 of raw or CHELEX-pretreated PVD$_{MnB1}$ in the presence or absence of Mn(III) after 20–24 h equilibration at 4°C: (1) PVD$_{MnB1}$-Mn(III) complex formed with 8.5 μM CHELEX-pretreated PVD$_{MnB1}$ and 30 μM Mn(III) added as citrate-Mn(III) (citrate-chelated Mn(III), section 2.1); (2) PVD$_{MnB1}$-Mn(III) complex formed with 8.1 μM raw PVD$_{MnB1}$ and 30 μM Mn(III) added as citrate-Mn(III); (3) PVD$_{MnB1}$-Mn(III) complex formed with 8.5 μM CHELEX-pretreated PVD$_{MnB1}$ and 50 μM Mn(III) acetate; (4) 8.1 μM raw PVD$_{MnB1}$; (5) EDTA-treated PVD$_{MnB1}$-Mn(III), initially formed by 20 h equilibration of 8.5 μM CHELEX-pretreated PVD$_{MnB1}$ and 30 μM Mn(III) (citrate-Mn(III)), followed by 10 h treatment with 10 mM EDTA; (6) 8.5 μM CHELEX-pretreated PVD$_{MnB1}$.
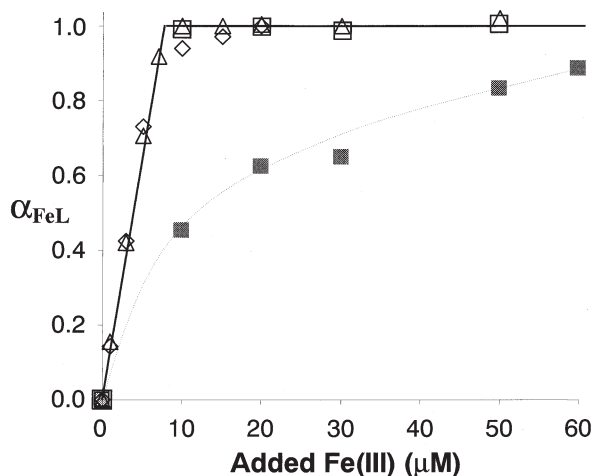
Fig. 3. Mole fraction (α_{FeL}) of PVD$_{MnB1}$-Fe(III) complex as a function of the concentration of citrate-Fe(III) added to 8.4–8.5 μM CHELEX-pretreated PVD$_{MnB1}$ at pH 8 and 4°C. Open diamonds: calculated from absorbance at 460 nm, 8.5 μM PVD$_{MnB1}$. Open triangles and squares: calculated from fluorescence quenching in two independent sets of measurements, one with 8.5 and one with 8.4 μM PVD$_{MnB1}$. The solid line through the data points represents the MINEQL+ forward simulation for citrate-Fe(III) added to 8.5 μM PVD$_{MnB1}$ at pH 8. Filled squares: varying concentrations of citrate-Fe(III) added in the presence of 10 μM Mn(III) (citrate-Mn(III)) and 8.4 μM PVD$_{MnB1}$, α_{FeL} calculated from absorbance at 460 nm. The dotted curve through the data points is a least-squares fit. Standard deviations of triplicate measurements were within the diameters of the symbols.

$$PVD - Fe + EDTA \rightarrow PVD + EDTA - Fe$$

$$K_{PE} = [PVD][EDTA - Fe]/[PVD - Fe][EDTA] \quad (6)$$

If the concentration of iron not bound by PVD or EDTA is negligible, then [EDTA-Fe] equals ($[Fe_{TOTAL}] - [PVD-Fe]$)

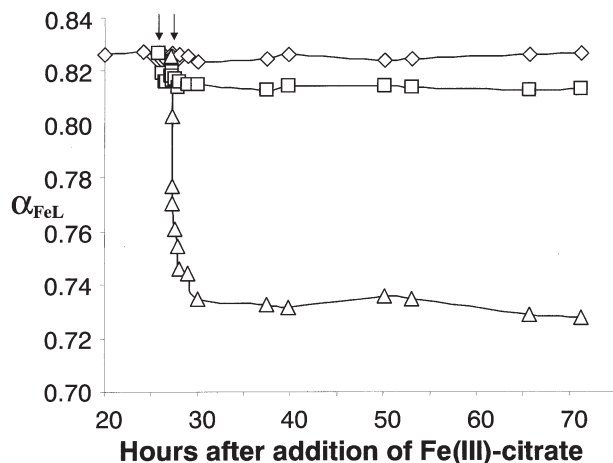
Fig. 4. Mole fraction (α_{FeL}) of PVD$_{MnB1}$-Fe(III) complex as a function of time after treatment with 1 or 10 mM EDTA. The complex was formed by combining 12 μM PVD$_{MnB1}$ and 10 μM Fe(III) (citrate-Fe(III)) at pH 8 in HEPES buffer (4°C), then challenged with 1 mM EDTA at 26 h or 10 mM EDTA at 27 h and further equilibrated at 4°C. Diamonds: no EDTA. Squares: 1 mM EDTA. Triangles: 10 mM EDTA. Standard deviations of triplicate fluorescence measurements were within the diameters of the symbols.

and the ligand concentrations, [EDTA] and [PVD], are each equal to the total concentration of the ligand added minus the concentration of its iron complex, making the determination of K$_{PE}$ facile (Meyer and Abdallah, 1978).

Reaction 6 represents two equilibria

$$EDTA + Fe \leftarrow \rightarrow EDTA - Fe$$

$$K_{EDTA} = [EDTA - Fe]/[EDTA][Fe] \quad (7)$$
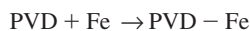
$$PVD + Fe \rightarrow PVD - Fe$$

$$K_{PVD} = [PVD - Fe]/[PVD][Fe] \quad (8)$$

where [Fe] is the concentration of Fe^{3+}. Therefore:

$$K_{PVD} = K_{EDTA}/K_{PE} \quad (9)$$

Based on the thermodynamic data for the Fe-EDTA system (Table 1) and the conditions in the competition experiments, $K_{EDTA} = 10^{23.57}$ M^{-1}. Our two measured values of K$_{PE}$ then lead to $K_{PVD} = 10^{28.6 \pm 0.3}$ M^{-1}. This value is larger than that reported for *P. fluorescens* (10^{27} M^{-1}; Meyer and Abdallah, 1978), but is in excellent agreement with that reported for *P. putida* strain BTP1 ($10^{29.2 \pm 0.5}$ M^{-1}, extrapolated to pH 8; Ongena et al., 2002), which produces an isopyoverdine having the peptide moiety attached to the number 3 carbon of the chromophore instead of the usual number 1 carbon.

Forward simulations (section 2.7) utilizing the MINEQL+ program (Schecher and McEvoy, 1998) with the thermodynamic constants in Table 1 indicated that the log stability constant of PVD$_{MnB1}$-Fe(III) extrapolated to zero ionic strength is 44.6 ± 0.5, a value somewhat higher than that of the typical pyoverdine of *P. aeruginosa* PaA (log K = 43.0 ± 0.3 at 25°C; Albrecht-Gary et al., 1994), but within the range of likely variation from procedural and microbial strain differences. Our estimate may be somewhat high because the constants in Table 1 could not be adjusted to 4°C due to unavailable standard enthalpy values.

3.3. Mn(III) Complex of PVD$_{MnB1}$

3.3.1. Absorbance and fluorescence

PVD$_{MnB1}$ samples exhibited similar absorption spectra after being exposed at pH 8 and 4°C to either Mn(III) acetate or citrate-chelated Mn(III) (citrate-Mn(III), section 2.1) (Fig. 2, curves 1 and 3). These spectra differed from those of samples treated with a parallel solution of citrate-chelated Fe(III) (Fig. 1, curve 1) or buffer without Mn or Fe (Fig. 2, curve 6). The PVD$_{MnB1}$-Mn(III) complexes absorbed maximally at 408–410 nm and did not show an absorption shoulder at 460 nm (Fig. 2, curves 1–3). The PVD$_{MnB1}$-Fe(III) complexes absorbed maximally at 400 nm and exhibited a pronounced shoulder at 460 nm (Fig. 1, curves 1–3), which is assigned as a charge transfer band of Fe bound to hydroxamate (Albrecht-Gary et al., 1994). Although the spectra of raw and CHELEX-pretreated PVD$_{MnB1}$ differed somewhat in the absence of Mn(III) (Fig. 2, curves 4 and 6), the spectra of the corresponding Mn(III) complexes were alike (Fig. 2, curves 1 and 2), suggesting that the other metal cations in raw PVD$_{MnB1}$ did not appreciably distort the spectrum of the Mn(III) complex. (Raw PVD$_{MnB1}$ differed from CHELEX-treated PVD$_{MnB1}$ in that divalent cations from the growth medium—
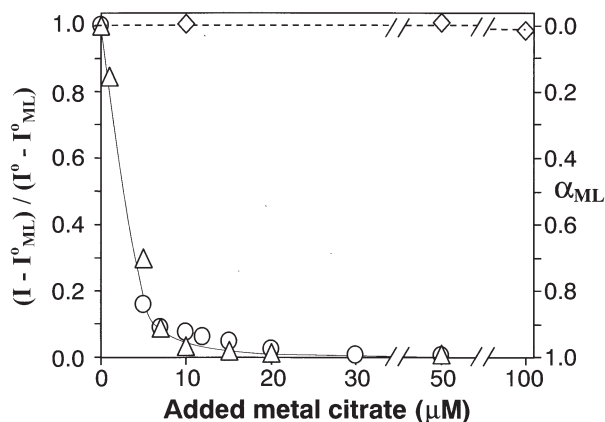
Fig. 5. Effect of varying concentrations of citrate-Fe(III), citrate-Mn(III), or citrate-Mn(II) on the relative fluorescence intensity of CHELEX-pretreated PVD_{MnB1} (8.5 μM) in 1 mM sodium citrate and HEPES buffer at pH 8 and 4°C. Triangles: citrate-Fe(III). Circles: citrate-Mn(III). Diamonds: citrate-Mn(II). Standard deviations of triplicate fluorescence measurements were within the diameters of the symbols. Lines are least squares fits to the data. The right axis shows the calculated mole fraction (α_{ML}) of PVD_{MnB1}-metal complex.

Fig. 6. Relative fluorescence at 4°C of PVD_{MnB1} (13.5 μM in HEPES buffer at pH 8) as a function of time after the addition of 50 μM Mn(III). Squares: relative fluorescence with Mn(III) acetate added. Diamonds: relative fluorescence with citrate-Mn(III) added. Standard deviations of triplicate fluorescence measurements were within the diameter of the symbols.

largely Mg^{2+} and Ca^{2+}—were exchanged for sodium during CHELEX treatment.)

Citrate-Mn(III) and citrate-Fe(III) similarly quenched the fluorescence of CHELEX-treated PVD_{MnB1} at pH 8 (Fig. 5). The break in shape in the quenching curve was at 8–10 μM Mn(III), close to the PVD_{MnB1} concentration of 8.5 ± 0.7 μM. No fluorescence quenching was seen in controls containing 10 mM sodium citrate (data not shown) or 100 μM Mn(II) added as its citrate chelate, citrate-Mn(II) (Fig. 5).

3.3.2. Citrate effects on the reaction of Mn(III) with PVD_{MnB1}

Fluorescence quenching of PVD_{MnB1} (concentration between 5 and 18 μM) by citrate-Mn(III) (Mn concentration between 5 and 50 μM) at pH 8 was complete in <2 h at 4°C. Figure 6 shows representative data for the reaction in HEPES buffer at pH 8 (4°C) of 13.5 μM PVD_{MnB1} with 50 μM Mn added as either citrate-Mn(III) or Mn(III) acetate.

The surprising result in Figure 6 was that the presence of citrate increased the apparent rate of the reaction; that is, citrate-Mn(III) (which has a citrate/Mn molar ratio of 20) had more effect at each time point than did Mn(III) acetate (which lacks citrate). A related result is that 2–3 times more added Mn(III) acetate than citrate-Mn(III) was needed to achieve metal saturation of PVD_{MnB1}, based on absorbance (Fig. 2, complete data set not shown). We interpret both observations to mean that citrate retarded the disproportionation or precipitation of Mn(III) (Klewicki and Morgan, 1998; Luther et al., 1998), thereby increasing the concentration of Mn(III) remaining in the reaction mixtures. We suspect that the stabilization of Mn(III) is the most important effect of citrate on Mn(III) in this system, especially since experiments in section 3.3.3 show that citrate can not compete effectively with PVD_{MnB1} for Mn(III) binding.

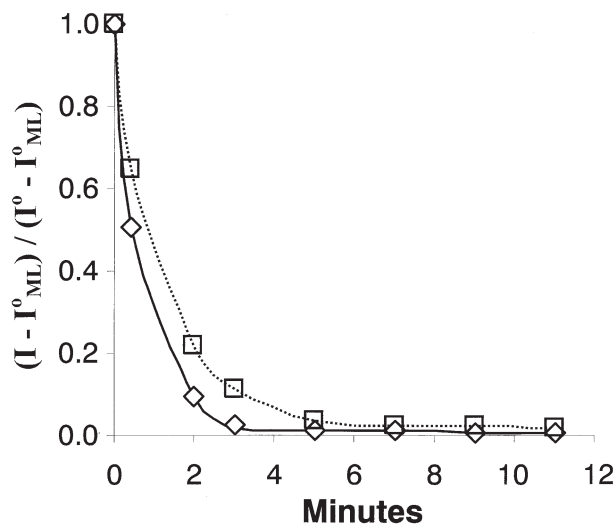The greater efficacy of citrate-Mn(III) than of Mn(III) ace-

tate in reactions with PVD_{MnB1} also provides indirect evidence that the addition of Mn(III), rather than an inadvertent Mn(IV) product of the disproportionation of Mn(III), was responsible for the bulk of the effects on fluorescence and absorbance that are described here. The 1:1 stoichiometry of the reaction of PVD_{MnB1} with Mn in citrate-Mn(III) (Fig. 3) also supports this contention.

3.3.3. Stability in the presence and absence of competing ligands or reductants

Excess citrate, a tricarboxylate ligand of metal ions, could not displace Mn(III) from its PVD_{MnB1} complex at pH 8 (4°C), as evidenced by the lack of any detectable change in the relative fluorescence when 10 mM citrate was added to a preformed PVD_{MnB1}-Mn(III) complex in the presence of 12 μM total PVD_{MnB1} (Fig. 7). In contrast, treatment with 1 or 10 mM pyrophosphate (conditions of 83- or 830-fold pyrophosphate excess relative to total PVD_{MnB1}) restored ~15% or 55%, of the quenched fluorescence, respectively, at 4°C (Fig. 7). Pyrophosphate-Mn(III) complexes slowly destabilize because of either Mn(III) disproportionation or ligand hydrolysis (Klewicki and Morgan, 1998) but are effective Mn(III) traps on short time scales at circumneutral pH (Kostka et al., 1995). Unfortunately, their stoichiometry and stability constants at pH 8 are not known (see Klewicki and Morgan, 1998) precluding a quantitative analysis of the data. Since pyrophosphate is thought to be among the strongest environmentally-prevalent ligands of Mn(III) (Kostka et al., 1995), the strong competition of PVD_{MnB1} with excess pyrophosphate for Mn(III) binding (Fig. 7) suggests that PVDs and perhaps certain other siderophores could be important ligands in natural Mn(III) chelation.

The fluorescence of preformed PVD_{MnB1}-Mn(III) complex was fully restored by treatment with 10 mM EDTA at either 21 h (data not shown) or 75 h after formation of the complex (Fig. 7, 4°C).
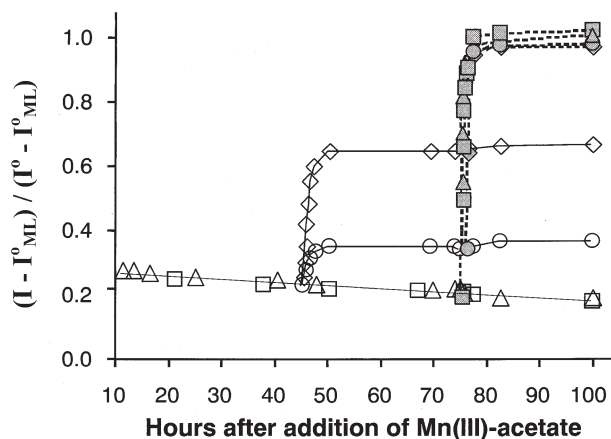
Fig. 7. Relative fluorescence of 12 μM PVD_{MnB1} reacted at pH 8 with 10 μM Mn(III) acetate, then exposed to competing ligands (pH 8, 4°C). Open triangles: no competitor. Filled triangles: 10 mM EDTA added at 75 h. Open squares: 10 mM sodium citrate added at 20 h. Filled squares: 10 mM EDTA added to half of the citrate-containing samples at 75 h. Open circles: 1 mM $Na_4P_2O_7$ added at 45.5 h. Closed circles: 10 mM EDTA added to half of the 1 mM $Na_4P_2O_7$-containing samples at 76 h. Open diamonds: 10 mM $Na_4P_2O_7$ added at 45.6 h. Closed diamonds: 10 mM EDTA added to half of the 10 mM $Na_4P_2O_7$-containing samples at 76 h.

Since EDTA-Mn(III) complexes rapidly undergo intramolecular electron transfer (Klewicki and Morgan, 1998), EDTA-mediated dissociation of PVD_{MnB1}-Mn(III) likely involves both chelation and reduction of Mn(III). One hour of exposure at 25°C to another reductant, 1 mM sodium ascorbate, reversed 64% of the fluorescence quenching in a sample containing 20 μM Mn(III) acetate and 12 μM raw PVD_{MnB1} in 67 mM HEPES buffer at pH 8. Taken together, these observations indicate that Mn(III) in its PVD_{MnB1} complex at pH 8 is accessible to reductants (ascorbate and EDTA) and to a high-affinity Mn(III) ligand that is not a reductant (pyrophosphate; Klewicki and Morgan, 1998), but not to a moderate-affinity carboxylate ligand (citrate, Table 1, β by analogy to Fe(III)).

That the Mn(III) complex of PVD_{MnB1} was quite stable in the absence of strong ligands or reductants was shown by the continued fluorescence quenching of that complex during 100 h at 4°C (Fig. 7). Mn(III) did not detectably decompose the PVD_{MnB1} at pH 8 since EDTA treatment restored both the full fluorescence (Fig. 7) and the original absorption spectrum (Fig. 2, curve 5) of PVD_{MnB1}. Furthermore, the ability to bind Fe(III) was not destroyed by Mn(III) exposure (see section 3.4 below).

3.4. Competition between Fe(III) and Mn(III) for PVD_{MnB1}

3.4.1. Simultaneous addition of citrate-Fe(III) and citrate-Mn(III)

Since absorbance at 460 nm of Fe(III)-saturated PVD_{MnB1} differs substantially from that of Mn(III)-saturated or untreated PVD_{MnB1} (Figs. 1 and 2), the value of α_{FeL} for a sample containing both Mn(III) and Fe(III) could be assessed from its A_{460} in comparison to parallel controls containing each metal alone. When varying concentrations of citrate-Fe(III) were added to 8.4 μM PVD_{MnB1} at 4°C, the value of α_{FeL} was
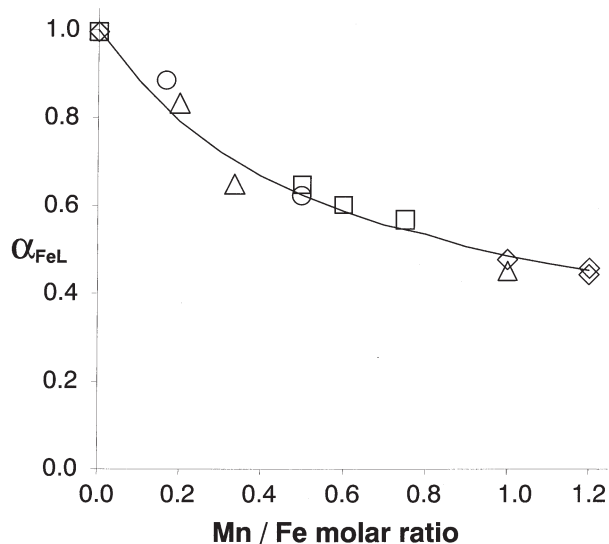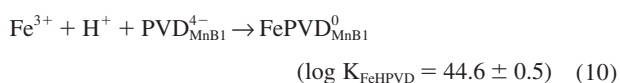

Fig. 8. Mole fraction of PVD_{MnB1}-Fe(III) complex (calculated from absorbance at 460 nm) as a function of the Mn/Fe molar ratio after the simultaneous addition of citrate-Fe(III) and citrate-Mn(III) to a CHELEX-treated culture filtrate containing 8.1 μM PVD_{MnB1} and 2 mM Na citrate in HEPES buffer at pH 8 (4°C). Diamonds: 10 μM Fe(III) with varying concentrations of Mn(III). Squares: 20 μM Fe(III) with varying concentrations of Mn(III). Triangles: 10 μM Mn(III) with varying concentrations of Fe(III). Circles: 20 μM Mn(III) with varying concentrations of Fe(III). The curve through the data points represents a MINEQL+ forward simulation of the system with 20 μM Fe(III) and varying concentrations of Mn(III).

strikingly smaller in the presence as compared to the absence of citrate-Mn(III) (lower curve in Fig. 3). With 10 μM Mn(III), α_{FeL} at 10 μM Fe(III) equaled 0.45 and Fe saturation could not be achieved even when 60 μM Fe(III) was added (lower curve in Fig. 3).

In a repeat experiment with 8.1 μM PVD_{MnB1} at 4°C, the value of α_{FeL} decreased with increasing citrate-Mn(III)/citrate-Fe(III) molar ratio (Fig. 8). The value of α_{FeL} was similar at the same Mn/Fe ratio, independently of whether the ratio was achieved with 10 or 20 μM Mn(III) and varying concentrations of Fe(III), or with 10 or 20 μM Fe(III) and varying concentrations of Mn(III) (Fig. 8). Absorption spectra of the same sample at 20 and 41 h equilibration were nearly identical (data not shown), indicating that equilibrium had been achieved by 20 h.

To calculate the stability constant of the Mn(III) complex of PVD_{MnB1}, we followed a two-step strategy: (1) determination of the stability constant of $FeHPVD_{MnB1}$ using forward simulation (section 3.2), and (2) analysis of the competition between Mn(III) and Fe(III) for PVD_{MnB1}. Our EDTA competition data could not be used to determine the stability of the PVD_{MnB1}-Mn(III) complex because the EDTA-Mn(III) complex is susceptible to intramolecular electron transfer (Klewicki and Morgan, 1998). We assumed the following complexation reactions:
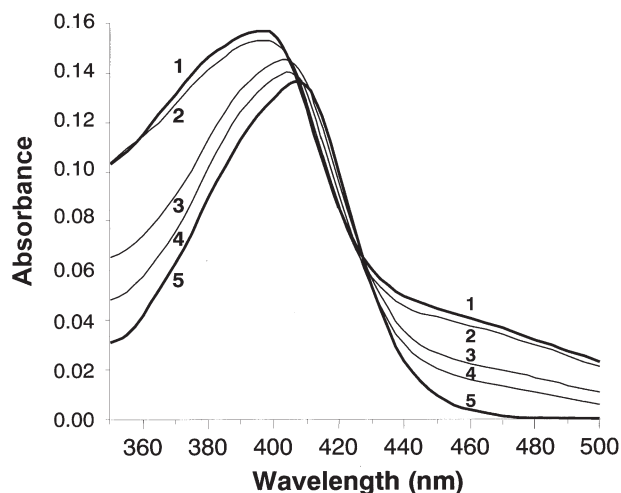
$$Fe^{3+} + H^+ + PVD_{MnB1}^{4-} \rightarrow FePVD_{MnB1}^0$$

$$(\log K_{FeHPVD} = 44.6 \pm 0.5) \quad (10)$$

$$Mn^{3+} + H^+ + PVD_{MnB1}^{4-} \rightarrow MnHPVD_{MnB1}^0$$

$$(\log K_{MnHPVD}) \quad (11)$$

Fig. 9. Absorption spectra of PVD_{MnB1} (8.1 μM) complexes with 20 μM Fe(III) and/or 20 μM Mn(III) after 41 h equilibration at 4°C and pH 8. Metals were supplied as citrate chelates: citrate-Mn(III) and citrate-Fe(III). (1) PVD_{MnB1}-Fe(III); (2) PVD_{MnB1}-Fe(III) to which Mn(III) was added after 20 h equilibration; (3) PVD_{MnB1} to which Fe(III) and Mn(III) were added simultaneously at 0 h; (4) PVD_{MnB1}-Mn(III) to which Fe(III) was added after 20 h equilibration; (5) PVD_{MnB1}-Mn(III).

A forward simulation (section 2.7) using MINEQL+ (Schecher and McEvoy, 1998) with the thermodynamic constants in Table 1 yielded the curve shown in Figure 8, which fits the data well and is based on log $K_{MnHPVD} = 47.5 \pm 0.5$ (extrapolated to zero ionic strength).

3.4.2. Sequential addition of citrate-Fe(III) and citrate-Mn(III)

In metal displacement experiments at 4°C, 10 μM Fe (citrate-Fe(III)) or 10 μM Mn (citrate-Mn(III)) was added to 8.1 μM PVD_{MnB1} at pH 8, followed by equimolar addition of the other metal after 20 h equilibration at 4°C. (Fig. 9). Values of α_{FeL}, calculated from A_{460} readings at 21 h of further equilibration, were ~0.9 if Fe(III) was added first and ~0.3 if Mn(III) was added first, as compared to 0.47 ± 0.02 if the two metals were added simultaneously (Table 3). The effect of the sequence of metal addition may have a trivial explanation related to differing final Mn(III) concentrations caused by the

Table 3. Effect on α_{FeL} at 4°C of sequential or simultaneous additions of 10 μM Fe(III) and 10 μM Mn(III) to 8.1 μM PVD_{MnB1}.

Added at 0 h	Added at 20 h	α_{FeL} at 19 h	α_{FeL} at 41 h
Fe	Mn	1.01[a]	0.88
Mn	Fe	0.00[a]	0.32
Fe + Mn	—[b]	0.46	0.45
Fe + Mn	—[b]	0.47	0.48
Fe	—[b]	0.99[a]	1.01
Mn	—[b]	0.00[a]	0.00

[a] A_{460} values of the two Fe-only samples at 19 h were averaged to estimate $\alpha_{FeL} = 1.00$; those of the two Mn-only samples at 19 h were averaged to estimate $\alpha_{FeL} = 0.00$.

[b] No metal addition at 20 h.

greater stability of PVD_{MnB1}-Mn(III) than citrate-Mn(III) to reduction and disproportionation of Mn(III) (Figure 7, with comparison to Klewicki and Morgan, 1998). Since the kinetic parameters of the citrate-Mn(III) reaction with PVD_{MnB1} and $FeHPVD_{MnB1}$ are not likely to be the same, the percentage of the reaction time during which the Mn(III) existed as citrate-Mn(III) vs. PVD_{MnB1}-Mn(III) undoubtedly differed in the two cases, affecting the rates of Mn(III) removal from the system by reduction or disproportionation. Also, the kinetics of metal association with or dissociation from PVD_{MnB1} may differ between Fe(III) and Mn(III). However, the current lack of kinetic information does not detract from the primary conclusions of this experiment, that: (a) either metal could displace the other from its PVD_{MnB1} complex, and (b) the final concentrations of the Fe(III) and Mn(III) complexes of PVD_{MnB1} at 41 h were both within the same order of magnitude (ranging from 1 to 7 μM) no matter the sequence of metal addition.

4. SUMMARY AND IMPLICATIONS

We have sought to examine the interaction of Mn(III) with PVD_{MnB1} under physiologically-relevant conditions: at pH 8 and in spent culture fluid. This fluid necessarily included cations that were required for bacterial growth and may possibly have contained additional chelators and siderophores, which are known to be produced by certain *Pseudomonas* sp. isolates (Budzikiewicz, 1993; Bultreys and Gheysen, 2000; Mossialos et al., 2000; Cornelis and Matthijs, 2002). Since the other reported siderophores of fluorescent pseudomonads have affinities for Fe(III) that are several orders of magnitude lower than those of PVDs (Budzikiewicz, 1993; Cornelis and Matthijs, 2002) and often are not synthesized in the presence of pyoverdines (Mossialos et al., 2000), they were not anticipated to interfere strongly in the current experiments. With respect to cations in the growth medium, MSP medium contains only mono- or divalent cations, which have much lower affinities for PVD than do trivalent ones (Hernlem et al., 1996). The inability of divalent cations to influence the fluorochromophore of PVD also arises because divalent ions predominantly contact the two hydroxamate groups of PVD, whereas trivalent ions bind the catecholate group as well as the hydroxamates; the fluorochromophore of PVD contains the catecholate but is distant from the hydroxamates and thus is expected to be preferentially influenced by chelate formation with trivalent ions (Albrecht-Gary et al., 1994). Furthermore, controls involving Mn^{2+} (section 3.3.1), the reducing agent ascorbate (section 3.3.3), EDTA (sections 3.1.1 and 3.3.1), and the ion exchange resin CHELEX-100 (sections 3.1.1 and 3.3.1), confirmed that divalent ions, either from the growth medium (largely Mg^{2+} and Ca^{2+}) or subsequently added (Mn^{2+}), had a very minimal effect on fluorochromophore-based studies of PVD_{MnB1}. This fortunate circumstance, combined with the facts that PVD and its trivalent metal chelates have large extinction coefficients and that PVD was the only detectable fluorochromophore that absorbed light at wavelengths >350 nm in strain MnB1 cultures (section 3.1.1), permitted investigation of the PVD component of the culture fluid without requiring substantial perturbation of the total system. Comparison to future studies with purified PVD may reveal minor contributions of other system

components, but this comparison can be made only if the total system is also examined, as it was here.

The salient conclusion of this paper is that Mn(III) competed strongly with Fe(III) for binding by PVD_{MnB1} (section 3.4). The stability constant (K_{MnHPVD}) of $MnHPVD_{MnB1}$, estimated from studies at 4°C involving various ratios of added Fe(III) and Mn(III) (Fig. 8) and extrapolated to zero ionic strength reference state, was $10^{47.5 \pm 0.5} M^{-1}$ (section 3.4.1), whereas the corresponding stability constant of $FeHPVD_{MnB1}$ was $10^{44.6 \pm 0.5} M^{-1}$ (section 3.2). That K_{MnHPVD} exceeds K_{FeHPVD} is not surprising, given that the affinities of metal cations for hydroxamate-containing siderophores correlate strongly and positively with each ion's first hydrolysis constant (Hernlem et al., 1996). The hydrolysis constants of Mn^{3+} are exceptionally large, surpassing those of Fe^{3+} by two to five orders of magnitude (Martell et al., 1998). We therefore expect that Mn^{3+} (affected by other chemical species of Mn(III) in any given system) will bind strongly to hydroxamate siderophores in general and compete effectively with Fe^{3+} or other cations. Desferrioxamine B, a trihydroxamate siderophore, has been shown to complex Mn^{3+} (Faulkner et al., 1994), although with an as-yet unknown affinity.

The accessibility of the Mn(III) in its PVD_{MnB1} complex was examined in reactions with various reductants or competing ligands, namely: ascorbate, which can reduce Mn(III) to Mn(II); EDTA, a high affinity ligand that is also a reductant because its Mn(III) complex is susceptible to rapid intramolecular electron transfer (Klewicki and Morgan, 1998); pyrophosphate (mainly $HP_2O_7^{3-}$ and $P_2O_7^{4-}$ at pH 8), a strong Mn(III) ligand that does not undergo electron transfer (Kostka et al., 1995; Klewicki and Morgan, 1998); and citrate, a moderate-strength ligand that can be oxidized by Mn(III) at low pH but is relatively stable at pH 8 (Klewicki and Morgan, 1998). That the PVD_{MnB1}-complexed Mn(III) was available to the two reductants (ascorbate and EDTA, section 3.3.3) suggests that this siderophore-Mn(III) complex likely can participate in environmentally important redox reactions. Since PVD_{MnB1}-Mn(III) only partially released its Mn(III) in competition with an 830-fold excess of pyrophosphate and was not detectably affected by excess citrate (Fig. 7) it seems probable that siderophore-Mn(III) complexes could be reservoirs of soluble Mn(III) in natural circumstances, as has been proposed for pyrophosphate (Kostka et al., 1995; Luther et al., 1998; Klewicki and Morgan, 1999).

Binding of Mn(III) by PVD_{MnB1} has three major biogeochemical implications involving: (a) intermediates and products of bacterial Mn(II) oxidation, (b) stabilization of soluble Mn(III), a strongly reactive species, in natural waters, and (c) competition between Mn(III) and Fe(III) for siderophore binding, with effects on iron bioavailability. Concerning the first topic, uncertainty has existed concerning whether bacterial Mn(II) oxidation proceeds via an Mn(III) intermediate (Mandernack et al., 1995a,b; Bargar et al., 2000), but current evidence that Mn(II) oxidation is catalyzed by multicopper oxidase-like proteins (van Waasbergen et al., 1996; Corstjens et al., 1997; Brouwers et al., 1999; Francis et al., 2001) suggests that such an intermediate exists (Tebo, 1998). Indeed, an Mn(III) intermediate in Mn(II) oxidation by the bacterium *Bacillus* sp. strain SG-1 has recently been observed via its pyrophosphate complex (Webb et al., 2002). Since PVD_{MnB1} binds Mn(III) more strongly than does pyrophosphate (Fig. 7),

pyoverdine likewise can be expected to prolong the life of Mn(III) and retard its oxidation to Mn(IV). This phenomenon could explain why the production of Mn(IV) oxides is delayed or even absent in *P. putida* cultures that are induced to synthesize pyoverdine or are constitutive pyoverdine-producing mutants (Caspi et al., 1998; De Vrind et al., 1998). Future studies may elucidate whether: (a) pyoverdines or other chelators of Mn(III) play a role in Mn(II) oxidation by *P. putida* and (b) all pyoverdines, or only those from Mn(II)-oxidizing strains, complex Mn(III) as strongly as does PVD_{MnB1}.

Manganese(III) binding by pyoverdine may also impact the oxidation state of soluble Mn in any iron-limited environment that contains fluorescent pseudomonads—prevalent organisms in soils, sediments, waters, and some human disease conditions. Determinations of Mn oxidation state in natural waters frequently rely on assays of total manganese in samples that are fractionated by filtration to yield soluble Mn (assumed to be Mn(II)) and particulate Mn (assumed to be mainly Mn(IV) oxide precipitates). However, chelated Mn(III) could pass though filters. Therefore, the oxidation state of soluble Mn in aqueous environments that contain microbially-produced chelators may need to be reinvestigated.

REFERENCES

Albrecht-Gary A.-M., Blanc S., Rochel N., Ocaktan A. Z., and Abdallah M. A. (1994) Bacterial iron transport: Coordination properties of pyoverdin PaA, a peptidic siderophore of *Pseudomonas aeruginosa*. *Inorg. Chem.* **33,** 6391–6402.

Albrecht-Gary A.-M. and Crumbliss A. L. (1998) Coordination chemistry of siderophores: Thermodynamics and kinetics of iron chelation and release. In *Metal Ions in Biological Systems*, Vol. 35. (ed. H. Sigel), pp. 239–327. Marcel Dekker.

Bargar J. R., Tebo B. M., and Villinski J. E. (2000) In situ characterization of Mn(II) oxidation by spores of the marine *Bacillus* sp. strain SG-1. *Geochim. Cosmochim. Acta* **64,** 2775–2778.

Blaser P. and Sposito G. (1987) Spectrofluorometric investigation of trace metal complexation by an aqueous chestnut leaf litter extract. *Soil Sci. Soc. Am. J.* **51,** 612–619.

Brouwers G.-J., de Vrind J. P. M., Corstjens P. L. A. M., Cornelis P., Baysse C., and de Vrind-de Jong E. W. (1999) *cum*A, a gene encoding a multicopper oxidase, is involved in Mn^{2+} oxidation in *Pseudomonas putida* GB-1. *Appl. Environ. Microbiol.* **65,** 1762–1768.

Brouwers G. J., Vijgenboom E., Corstjens P. L. A. M., and deVrind-deJong E. W. (2000) Bacterial Mn^{2+} oxidizing systems and multicopper oxidases: An overview of mechanisms and functions. *Geomicrobiol. J.* **17,** 1–24.

Budzikiewicz H. (1993) Secondary metabolites from fluorescent pseudomonads. *FEMS Microbiol. Rev.* **104,** 209–228.

Bultreys A. and Gheysen I. (2000) Production and comparison of peptide siderophores from strains of distantly related pathovars of *Pseudomonas syringae* and *Pseudomonas viridiflave* LMG 2352. *Appl. Environ. Microbiol.* **66,** 325–331.

Call H. P. and Mucke I. (1997) History, overview and applications of mediated lignolytic systems, especially laccase-mediator-systems. (Lignozym(R)-process). *J. Biotechnol.* **53,** 163–202.

Caspi R., Tebo B. M., and Haygood M. G. (1998) c-Type cytochromes and manganese oxidation in *Pseudomonas putida* MnB1. *Appl. Environ. Microbiol.* **64,** 3549–3555.

Cornelis P. and Matthijs S. (2002) Diversity of siderophore-mediated iron uptake systems in fluorescent pseudomonads: Not only pyoverdines. *Environ. Microbiol.* **4,** 787–798.

Corstjens P. L. A. M., de Vrind J. P. M., Goosen T., and de Vrind-de Jong E. W. (1997) Identification and molecular analysis of the *Leptothrix discophora* SS-1 *mof*A gene, a gene putatively encoding a manganese oxidizing protein with copper domains. *Geomicrobiol. J.* **14,** 91–108.

De Vrind J. P., Brouwers G. J., Corstjens P. L. A. M., Den Dulk J., and De Vrind-De Jong E. W. (1998) The cytochrome c maturation operon is involved in manganese oxidation in *Pseudomonas putida* GB-1. *Appl. Environ. Microbiol.* **64,** 3556–3562.

Demange P., Wendenbaum S., Bateman A., Dell A. and Abdallah M. A. (1987) Bacterial siderophores: Structure and physicochemical properties of pyoverdins and related compounds. In *Iron Transport in Microbes, Plants and Animals* (ed. J. B. Neilands), pp. 167–187. VCH Press.

Dutton M. V. and Evans C. S. (1996) Oxalate production by fungi: Its role in pathogenicity and ecology in the soil environment. *Can. J. Microbiol.* **42,** 881–895.

Faulkner K. M., Stevens R. D., and Fridovich I. (1994) Characterization of Mn(III) complexes of linear and cyclic desferrioxamines as mimics of superoxide dismutase activity. *Arch. Biochem. Biophys.* **310,** 341–346.

Folschweiller N., Gallay J., Vincent M., Abdallah M. A., Pattus F., and Schalk I. J. (2002) The interaction between pyoverdin and its outer membrane receptor in *Pseudomonas aeruginosa* leads to different conformers: A time-resolved fluorescence study. *Biochemistry* **41,** 14591–14601.

Francis C. A., Co E.-M., and Tebo B. M. (2001) Enzymatic manganese(II) oxidation by a marine α-proteobacterium. *Appl. Environ. Microbiol.* **67,** 4024–4029.

Francis C. A. and Tebo B. M. (2001) *cumA* multicopper oxidase genes from diverse Mn(II)-oxidizing and non-Mn(II) oxidizing *Pseudomonas* strains. *Appl. Environ. Microbiol.* **67,** 4272–4278.

Francis C. A., Casciotti K., and Tebo B. M. (2002) Localization of Mn(II)-oxidizing activity and its putative multicopper oxidase, MnxG, to the exosporium of the marine *Bacillus* sp. strain SG-1. *Arch. Microbiol.* **178,** 450–456.

Hatakka A. (1994) Lignin-modifying enzymes from selected white-rot fungi: Production and role in lignin degradation. *FEMS Microbiol. Rev.* **13,** 12519.

Hatakka A., Lundell T., Hofrichter M., and Maijala P. (2003) Manganese peroxidase and its role in the degradation of wood lignin. *ACS Symposium Ser.* **855,** 230–243.

Hernlem B. J., Vane L. M., and Sayles G. D. (1996) Stability constants for complexes of the siderophore desferrioxamine B with selected heavy metal cations. *Inorgan. Chim. Acta* **244,** 179–184.

Kisaalita W. S., Slininger P. J., and Bothast R. J. (1997) Kinetic fluorometry of the iron-pyoverdine complex in acetate buffer media. *Biotechnol. Techniques* **11,** 649–651.

Klewicki J. K. and Morgan J. J. (1998) Kinetic behavior of Mn(III) complexes of pyrophosphate, EDTA and citrate. *Environ. Sci. Technol.* **32,** 2916–2922.

Klewicki J. K. and Morgan J. J. (1999) Dissolution of β-MnOOH particles by ligands: Pyrophosphate, ethylenediaminetetraacetate and citrate. *Geochim. Cosmochim. Acta* **63,** 3017–3024.

Kostka J. E., Luther G. W. III, and Nealson K. H. (1995) Chemical and biological reduction of Mn(III)-pyrophosphate complexes: Potential importance of dissolved Mn(III) as an environmental oxidant. *Geochim. Cosmochim. Acta* **59,** 885–894.

Leonowicz A., Cho N. S., Luterek J., Wilkolazka A., Wojtas-Wasilewska M., Matuszewska A., Hofrichter M., Wesenberg D., and Rogalski J. (2001) Fungal laccase: Properties and activity on lignin. *J. Basic Microbiol.* **41,** 185–227.

Luther G. W. III, Ruppel D. T., and Burkhard C. (1998) Reactivity of dissolved Mn(III) complexes and Mn(IV) species with reductants: Mn redox chemistry without a dissolution step. In *Mineral-Water Interfacial Reactions: Kinetics and Mechanisms*, ACS Symposium

Series Vol. 715 (ed. T. J. Grundl), pp. 265–280. American Chemical Society.

Mandernack K. W., Fogel M. L., Tebo B. M., and Usui A. (1995a) Oxygen isotope analyses of chemically and microbially produced manganese oxides and manganates. *Geochim. Cosmochim. Acta* **59,** 4409–4425.

Mandernack K. W., Post J., and Tebo B. M. (1995b) Manganese mineral formation by bacterial spores of the marine *Bacillus*, strain SG-1: Evidence for the direct oxidation of Mn(II) to Mn(IV). *Geochim. Cosmochim. Acta* **59,** 4393–4408.

Martell A. E., Smith R. M., and Motekaitis R. J. (1998) *Critically Selected Stability Constants of Metal Complexes Database.* National Institute of Standards and Technology.

Meyer J.-M. and Abdallah M. A. (1978) The fluorescent pigment of *Pseudomonas fluorescens:* Biosynthesis, purification and physiochemical properties. *J. Gen. Microbiol.* **197,** 319–328.

Meyer J.-M. (2000) Pyoverdines: Pigments, siderophores and potential taxonomic markers of fluorescent *Pseudomonas* species. *Arch. Microbiol.* **174,** 135–142.

Mossialos D., Meyer J.-M., Budsikiewics H., Wolff U., Koedam N., Baysse C., Anjaiah V., and Cornelis P. (2000) Quinolobactin, a new siderophore of *Pseudomonas fluorescens* ATCC 17400, the production of which is repressed by the cognate pyoverdine. *Appl. Environ. Microbiol.* **66,** 487–492.

Nealson K. H., Tebo B. M., and Rosson R. A. (1988) Occurrence and mechanisms of microbial oxidation of manganese. *Adv. Appl. Microbiol.* **33,** 279–318.

Nealson K. H., Rosson R. A. and Myers C. R. (1989) Mechanisms of oxidation and reduction of manganese. In *Metal Ions and Bacteria* (ed. R. J. Doyle), pp. 383–411. Wiley.

Ongena M., Jacques P., Delfosse P., and Thonart P. (2002) Unusual traits of the pyoverdine-mediated iron acquisition system in *Pseudomonas putida* BTP1. *Biometals* **15,** 1–13.

Perie F. H. and Gold M. H. (1991) Manganese regulation of manganese peroxidase expression and lignin degradation by the white rot fungus *Dichomitus squalens*. *Appl. Environ. Microbiol.* **57,** 2240–2245.

Popp J. L., Kalyanaraman B., and Kirk T. K. (1990) Lignin peroxidase oxidation of Mn^{+2} in the presence of veratryl alcohol, malonic or oxalic acid and oxygen. *Biochemistry* **29,** 10475–10480.

Ribas X., Salvadó V., and Valiente M. (1989) The chemistry of iron in biosystems. Part 2. A hydrolytic model of the complex formation between iron(III) and citric acid in aqueous solutions. *J. Chem. Res. M* **1989,** 2533–2553.

Ryan D. K. and Weber J. H. (1982) Fluorescence quenching titration for the determination of complexing capacities and stability constants. *Anal. Chem.* **54,** 986–990.

Schalk I. J., Abdallah M. A., and Pattus F. (2002) Recycling of pyoverdin on the FpvA receptor after ferric pyoverdin uptake and dissociation in *Pseudomonas aeruginosa*. *Biochemistry* **41,** 1663–1671.

Schecher W. D. and McEvoy D. C. (1998) *MINEQL+, a Chemical Equilibrium Modeling System.* Environmental Research Software.

Schlosser D. and Hofer C. (2002) Laccase-catalyzed oxidation of Mn^{2+} in the presence of natural Mn^{3+} chelators as a novel source of extracellular H_2O_2 production and its impact on manganese peroxidase. *Appl. Environ. Microbiol.* **68,** 3514–3521.

Schweisfurth R. (1973) Manganoxydierende Bakterien. I. Isolierung und Bestimmung einiger Stamme von Manganbakterien. *Z. Allg. Mikrobiol.* **13,** 341–347.

Sposito G. (1989) *The Chemistry of Soils.* Oxford University Press.

Stone A. T. (1987) Microbial metabolites and the reductive dissolution of manganese oxides: Oxalate and pyruvate. *Geochim. Cosmochim. Acta* **51,** 919–925.

Stumm W. and Morgan J. J. (1996) *Aquatic Chemistry*. Wiley.

Tebo B. M. (1998) Comment on the comment of A. W. M. G. Souren on "Oxidation of cobalt and manganese in seawater via a common microbially catalyzed pathway". *Geochim. Cosmochim. Acta* **62,** 357–358.

Tebo B. M., Ghiorse W. C., van Waasbergen L. G., Siering P. L., and Caspi R. (1997) Bacterially mediated mineral formation: Insights into manganese(II) oxidation from molecular genetic and biochemical studies. *Rev. Mineral.* **35,** 225–266.

van Waasbergen L. G., Hoch J. A., and Tebo B. M. (1993) Genetic analysis of the marine manganese-oxidizing *Bacillus* sp. strain SG-1: Protoplast transformation Tn917 mutagenesis and the identification of chromosomal loci involved in manganese oxidation. *J. Bacteriol.* **175,** 7594–7603.

van Waasbergen L. G., Hildebrand M., and Tebo B. M. (1996) Identification and characterization of a gene cluster involved in manganese oxidation of spores of the marine *Bacillus* sp. strain SG-1. *J. Bacteriol.* **178,** 3517–3530.

Villalobos M., Toner B., Bargar J., and Sposito G. (2003) Characterization of the manganese oxide produced by *Pseudomonas putida* strain MnB1. *Geochim. Cosmochim. Acta* **67,** 2649–2662.

Webb S. M., Bargar J. R., and Tebo B. M. (2002) Existence of intermediate Mn(III) species in the microbially mediated oxidation of Mn(II). *Abst. Papers Amer. Chem. Soc.* 223:U601.

Xyla A. G., Sulzberger B., Luther G., Hering J. G., van Cappellan P., and Stumm W. (1992) Reductive dissolution of manganese(III,IV). (Hydr)oxides by oxalate: The effects of pH and light. *Langmuir* **8,** 95–103.